Robotica (2004) volume 22, pp. 567–576. © 2004 Cambridge University Press
DOI: 10.1017/S0263574704000323 Printed in the United Kingdom

A stiffness analysis for a hybrid parallel-serial manipulator

Giuseppe Carbone and Marco Ceccarelli

Laboratory of Robotics and Mechatronics, DiMSAT – University of Cassino, Via Di Biasio 43, 03043 Cassino (Fr) (Italy)
E-mail: carbone@unicas.it; ceccarelli@unicas.it

(Received in Final Form: February 3, 2004)

SUMMARY
In this paper a hybrid parallel-serial manipulator, named as CaHyMan (Cassino Hybrid Manipulator), is analyzed in term of stiffness characteristics as a specific example of a general procedure for analyzing stiffness of parallel-serial manipulators. A formulation is presented to deduce the stiffness matrix as a function of the most important stiffness and design parameters of the mechanical design. A formulation is proposed for a stiffness performance index by using the obtained stiffness matrix. A numerical investigation has been carried out on the effects of design parameters and fundamental results are discussed in the paper.

KEYWORDS: Stiffness analysis; Hybrid manipulator; Design parameters

1. INTRODUCTION

Usually, industrial robots are made in accordance with a serial manipulator architecture.[1–4] Robots having this type of architecture suffer from several known drawbacks, such as relatively low stiffness and accuracy, low nominal load/weight ratio and heavy structure. Therefore, in the last two decades many researchers have investigated the use of parallel architecture robots in order to obtain better performance. Some of the advantages of robots having parallel structure are the low weight, compact structure, better accuracy and stiffness, as stressed in reference [5]. Nevertheless, this type of robotic architecture also suffers from some drawbacks, such as a small workspace when compared with the dimension of the robot a complex mechanical design difficult Kinematics and, sometimes, a presence of singularities inside the workspace. Therefore, in the last decade hybrid manipulators have given great attention to robotic manipulators that are a combination of serial and parallel chain architectures. Some significant examples of hybrid manipulators are: ARTISAN from Stanford University (USA),[6] HRM from Korea Institute of Machinery and Materials (Korea),[7] GEORGV from the Institute of Production Engineering and Machine Tools (Germany),[8] and UPSarm from the California University at Davis (USA).[9] Other prototypes of hybrid manipulators have been also proposed by Shahinpoor,[10] Romdhane,[11] Kim et al.,[12] Nazarczuk et al.,[13] Huang and Ling,[14] Zanganeh and Angeles,[15] and Wuang.[16]

Combining serial and parallel chains in these manipulators offers the possibility, of having the advantages of both architectures and reduce their drawbacks. In particular, a hybrid manipulator can have an accuracy comparable with a parallel manipulator, and a workspace comparable with a serial manipulator. In order to obtain this result, a designer should compute the expected workspace and accuracy performances through a workspace and stiffness analysis, and she/he then should verify if these performances are suitable for the specific tasks for which the manipulator has been designed. It is worthy noting that a stiffness analysis is needed since it is related to accuracy properties. In fact, if the stiffness of links and joints are inadequate, external forces and moments may cause large deflections in the links bodies, which are undesirable from the viewpoint of both accuracy and payload performances.

The stiffness properties of a manipulator can be defined through a 6×6 matrix that is called a stiffness matrix K. This matrix gives the relationship between the vector of the compliance displacements of the end effector when a static wrench acts upon it, and the wrench itself. The stiffness matrix can be numerically computed by defining a suitable model of the manipulator, which takes into account the stiffness properties of each element of the manipulator and, in particular, the lumped stiffness parameters of links and motors. Examples of how the model of a manipulator can be developed are proposed in references [17–24].

In this paper the hybrid manipulator, named CaHyMan (Cassino Hybrid Manipulator), is analyzed in term of stiffness characteristics by developing a suitable model, and a formulation is proposed to deduce the stiffness matrix as a function of the most important stiffness parameters of the mechanical design. Although the approach can be adopted by general procedures, the proposed formulation and analysis are specific for a specific architecture in order to give an effective practical application to the stiffness analysis of hybrid manipulators.

2. CaHyMAN ARCHITECTURE

The hybrid manipulator named as CaHyMan (Cassino Hybrid Manipulator) has been designed and built at the Laboratory of Robotics and Mechatronics in Cassino (Italy). This prototype (Figs. 1 and 2) is based on the mechanical design of a built prototype of CaPaMan (Cassino Parallel Manipulator),[25,26] by adding to it a telescopic arm. In particular, the telescopic arm is installed on the mobile plate MP of CaPaMan. The aim of this assembly is that the parallel architecture will work as an intelligent complaint base for the telescopic arm, which will operate in a static or quasi-static state for *a priori* determined task.

Fig. 1. The built prototype of CaHyMan (Cassino Hybrid Manipulator) at Laboratory of Robotics and Mechatronics in Cassino.

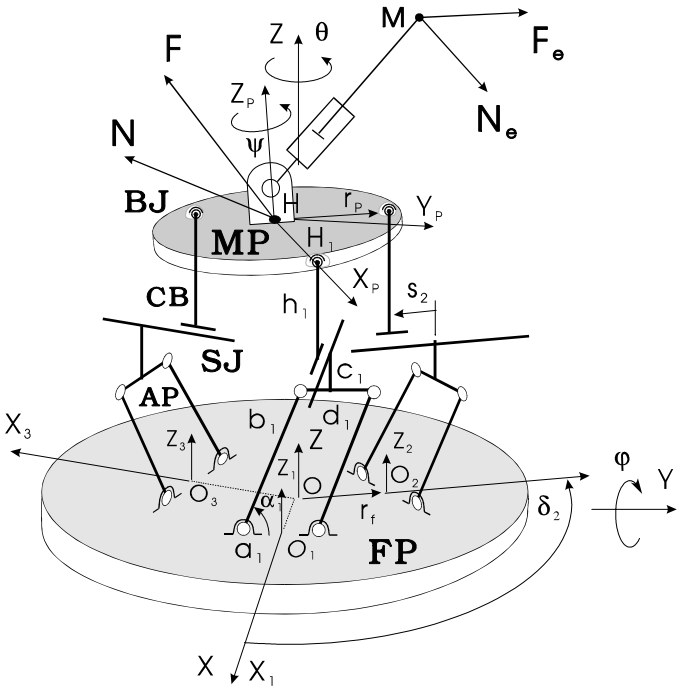

Fig. 2. Kinematic chain and design parameters for the parallel–serial hybrid manipulator CaHyMan.

The CaPaMan prototype is composed of a movable plate MP, which is connected to a fixed plate FP by means of three leg mechanisms. Each leg mechanism is composed of an articulated parallelogram AP whose coupler carries a prismatic joint SJ, a connecting bar CB, which transmits the motion from AP to MP through SJ, and a spherical joint BJ, which is installed on MP. The sizes of MP and FP are given by r_p and r_f, respectively (Fig. 2).

The telescopic arm is composed of a prismatic joint, a connecting bar and a revolute joint.

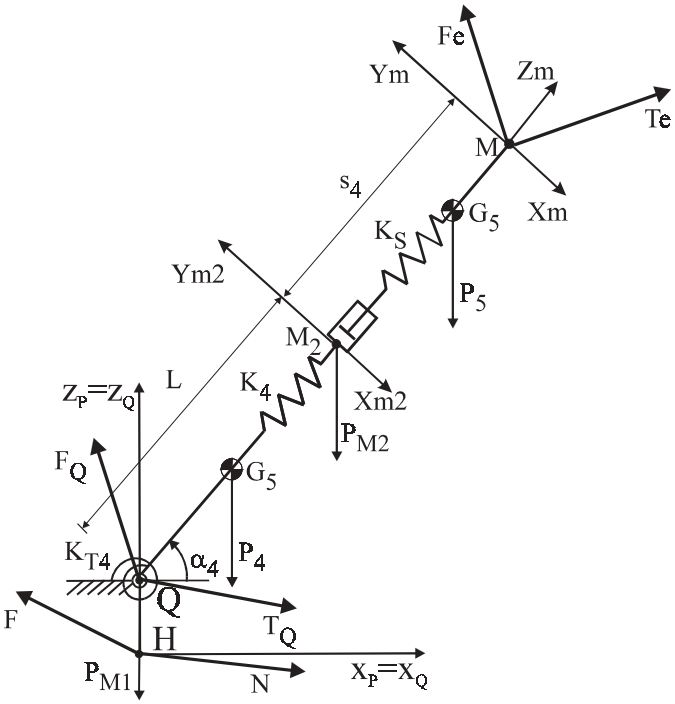

Fig. 3. A scheme for the evaluation of static equilibrium and stiffness matrix in the serial sub-chain of CaHyMan.

The design parameters for the parallel-serial manipulator CaHyMan are (k = 1, 2, 3): $a_k = c_k$, $b_k = d_k$, links of the k-th leg mechanism; h_k, the length of the connecting bar; α_κ, the input crank angle; s_k, the stroke of the prismatic joint; HM, the length of the telescopic arm; s_4 the stroke of the prismatic joint of the telescopic arm; α_4 the revolute joint angle; and λ, the angle, that locates the telescopic arm frame with respect to the mobile frame $X_pY_pZ_p$.

Reference frames have been fixed to the points M, M_2 and Q on the telescopic arm giving $X_mY_mZ_m$, $X_{m2}Y_{m2}$ Z_{m2}, $X_QY_QZ_Q$ frames, respectively, as shown in Fig. 3. The fixed frame XYZ has been fixed to the point O on the FP.

The prototype of CaHyMan is actuated by three dc motors installed on CaPaMan; another dc motor for α_4 motion and a step motor for s_4 motion are installed on the telescopic arm.

3. STIFFNESS CHARACTERISTICS OF CAHYMAN

The stiffness characteristics of CaHyMan are related to those of the links, joints and actuators. Referring to the mechanical design of Figs. 1 and 2 the mechanical system can be modelled by lumped parameters for each component, as shown in Figs. 3 and 4.

Referring to the telescopic arm of Fig. 3 the stiffness parameters are indicated as K_s for the prismatic joint and the step motor, K_4 for the connecting bar, K_{T4} for the dc motor installed on the telescopic arm. Referring to a leg of CaPaMan of Fig. 4, the stiffness parameters are indicated as k_{bk} for the crank link, k_{dk} for the driven link, k_{ck} for the coupler link, k_{hk} for the connecting coupler rod and k_{Tk} for the actuating system. The crank link b_k can be modelled as a beam so that stiffness can be evaluated through equivalent axial stiffness coefficient k_{bk}, which describes link axial

https://doi.org/10.1017/S0263574704000323 Published online by Cambridge University Press

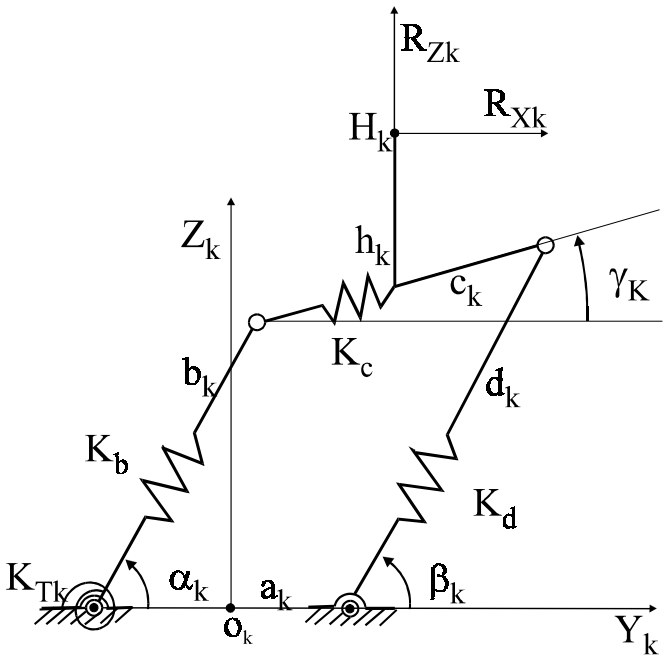

Fig. 4. A scheme for the stiffness evaluation of a CaHyMan leg.

stiffness and support radial stiffness. The parameter k_{Tk} can take into account the flexural stiffness of the crank link and the torsion stiffness of bearing, transmission and actuator. The driven link d_k behaves as a rod and its stiffness can be suitably described by the coefficient k_{dk}, which takes into account the axial stiffness of the link and radial stiffness of the joints only. The coupler link c_k carries the prismatic sliding joint that frees the parallelogram of transversal force components. Thus, the coupler link may have flexion deformation. Nevertheless, its stiffness coefficient k_{ck} can be considered due only to axial stress since the link is designed for flexion rigidity. In fact, generally the coupler link can be considered not deformable since it is massive in order to ensure no flexion deformation for payload capability and high precision positioning of CaHyMan (see the prototype of Fig. 1). However k_{ck} can be used to consider conveniently the stiffness of the coupler link and transversal compliance of the sliding joint unit.

Because of the ball joint SJ in the mechanical design of CaHyMan mobile plate, only a force acts on each CaHyMan leg. This force lays in the plane of the parallelogram with components R_{ky} and R_{kz}, according to the scheme of Fig. 4, since R_{kx} makes the prismatic joint slide or gives a negligible transversal flexion stress to the leg structure at a static configuration. Therefore k_{hk} describes mainly the axial stiffness of the connecting rod and radial stiffness of the joints, although it may take into account the compliance of the prismatic guide when the sliding joint works at its extremity.

4. STIFFNESS MATRIX OF CAHYMAN

The compliant displacement $\Delta\mathbf{X}_{\text{CaHyMan}}$ of the hybrid manipulator CaHyMan can be computed as the sum of $\Delta\mathbf{X}_{\text{PAR}}$ and $\Delta\mathbf{X}_{\text{SER}}$ compliant displacements in the parallel and serial manipulators, respectively. The compliant displacements are due to the action $\mathbf{F_M} = (\mathbf{F_e}, \mathbf{N_e})$ of external force $\mathbf{F_e}$ and torque $\mathbf{N_e}$ acting on the extremity of the manipulator, Fig. 2. Therefore the compliant displacement can be expressed as

$$\Delta\mathbf{X}_{\text{CaHyMan}} = \Delta\mathbf{X}_{\text{PAR}} + \Delta\mathbf{X}_{\text{SER}} \tag{1}$$

where

$$\begin{aligned} \Delta\mathbf{X}_{\text{PAR}} &= \mathrm{K}_{\text{PAR}}^{-1} \quad \mathrm{M}_{\text{FT}} \quad \mathbf{F}_{\text{M}} \\ \Delta\mathbf{X}_{\text{SER}} &= \mathrm{K}_{\text{SER}}^{-1} \quad \mathbf{F}_{\text{M}} \end{aligned} \tag{2}$$

in which K_{PAR} and K_{SER} are the 6×6 stiffness matrix for the parallel and serial manipulators when they are described with respect to $X_PY_PZ_P$ frame.

Thus, the stiffness matrix of CaHyMan can be written as

$$\mathrm{K}_{\text{CaHyMan}}^{-1} = \mathrm{K}_{\text{PAR}}^{-1}\mathrm{M}_{\text{FT}} + \mathrm{K}_{\text{SER}}^{-1} \tag{3}$$

This gives the possibility to compute separately the matrices K_{PAR} and K_{SER}.

4.1. The stiffness matrix of the serial manipulator

The stiffness behavior of the serial manipulator depends on the following parameters, Fig. 3: K_4, the stiffness of the QM_2 link; K_S, the stiffness of the linear motor and MM_2 link; K_{T4}, the stiffness of motor located in Q.

The scheme of Fig. 3 can be considered to give the stiffness matrix from

$$\mathrm{K}_{\text{SER}} = \mathrm{R}_{\text{SP}} \quad \mathrm{K}_{\text{SS}} \quad \mathrm{As}^{-1} \tag{4}$$

by using matrices R_{SP}, K_{SS}, A_S whose elements can be computed separately by means of the following expressions:

- Matrix R_{SP}, which is the 6×6 matrix that describes the mobile frame $X_pY_pZ_p$ with respect to the fixed frame XYZ, can be given as

$$\mathrm{R}_{\text{SP}} = \begin{bmatrix} \mathrm{R}_{\text{PAR}} & 0 \\ 0 & 1 \end{bmatrix} \tag{5}$$

with I as identity 3×3 matrix. R_{PAR} describes the orientation of the mobile frame $X_PY_PZ_P$ with respect to the fixed frame XYZ in term of the Euler angles φ, θ and ψ for the parallel chain. R_{PAR} can be expressed as

$$\mathrm{R}_{\text{PAR}} = \begin{bmatrix} -\mathrm{s}\theta\,\mathrm{s}\psi + \mathrm{s}\varphi\,\mathrm{c}\theta\,\mathrm{c}\psi & -\mathrm{s}\theta\,\mathrm{c}\psi - \mathrm{s}\varphi\,\mathrm{c}\theta\,\mathrm{s}\psi & \mathrm{c}\theta\,\mathrm{c}\varphi \\ \mathrm{c}\theta\,\mathrm{s}\psi + \mathrm{s}\varphi\,\mathrm{s}\theta\,\mathrm{c}\psi & \mathrm{c}\theta\,\mathrm{c}\psi - \mathrm{s}\varphi\,\mathrm{s}\theta\,\mathrm{s}\psi & \mathrm{s}\theta\,\mathrm{c}\varphi \\ -\mathrm{c}\varphi\,\mathrm{c}\psi & \mathrm{c}\varphi\,\mathrm{s}\psi & \mathrm{s}\psi \end{bmatrix} \tag{6}$$

in which $c\theta = \cos\theta$, $s\theta = \sin\theta$ and so on.

- Matrix Kss is the stiffness matrix that gives the external forces and torques applied in M, Fig. 3, to have the compliant displacements ΔL, Δs_4 and $\Delta\alpha_4$. Referring to the model of Fig. 3, the following equations can be

https://doi.org/10.1017/S0263574704000323 Published online by Cambridge University Press

written

$$\begin{aligned} &F_{ex} - K_4 \Delta L c\alpha_4 - K_s \Delta s_4 c\alpha_4 \\ &\quad + [K_{T4}/(L + s_4)]\Delta\alpha_4 s\alpha_4 = 0 \\ &F_{ey} - K_4 \Delta L s\alpha_4 - K_s \Delta s_4 s\alpha_4 \\ &\quad + [K_{T4}/(L + s_4)]\Delta\alpha_4 c\alpha_4 = 0 \\ &T_{ey} - K_{T4}\Delta\alpha_4 = 0 \end{aligned} \tag{7}$$

By using Eq. (7), the Kss matrix can be expressed as

$$Kss = \begin{bmatrix} K_4 c\alpha_4 & K_s c\alpha_4 & -[K_{T4}/(L + s_4)]s\alpha_4 \\ K_4 s\alpha_4 & K_s s\alpha_4 & [K_{T4}/(L + s_4)]c\alpha_4 \\ 0 & 0 & K_{T4} \end{bmatrix} \tag{8}$$

- Matrix As, which is the matrix for converting compliant displacements ΔL, Δs_4, $\Delta\alpha_4$, in the links to displacements coordinates, in the form

$$A_s = \begin{bmatrix} c\alpha_4 & c\alpha_4 & -(L + s_4)s\alpha_4 \\ s\alpha_4 & s\alpha_4 & (L + s_4)c\alpha_4 \\ 0 & 0 & 1 \end{bmatrix} \tag{9}$$

Therefore, the stiffness matrix K_{SER} of Eq. (4) can be computed straightforward by using Eqs. (5) to (9).

4.2. The stiffness matrix of the parallel manipulator

The stiffness matrix K_{PAR} of the parallel manipulator can be deduced following the procedure that has been outlined for the CaPaMan prototype in a previous work.[23] Nevertheless, it is necessary to point out that for the CaHyMan the application point of external force $\mathbf{F_e}$ and torque $\mathbf{T_e}$ is in the point M (Fig. 2). Therefore, the reactions $\mathbf{F}$ and $\mathbf{N}$ at the frame joint of the serial manipulator can be considered as an external force and torque for the parallel manipulator. The matrix M_{FT} giving $\mathbf{F}_H = (\mathbf{F}, \mathbf{N})$ as function of $\mathbf{F}_M = (\mathbf{F}_e, \mathbf{T}_e)$ can be written in the form

$$M_{FT} = \begin{bmatrix} -s\alpha_4 & 0 & -c\alpha_4 & 0 & 0 & 0 \\ 0 & -1 & 0 & 0 & 0 & 0 \\ c\alpha_4 + \frac{C_1}{F_{ex}} & \frac{C_1}{F_{ey}} & -s\alpha_4 + \frac{C_1}{F_{ez}} & \frac{C_2}{T_{ex}} & \frac{C_2}{T_{ey}} & \frac{C_2}{T_{ez}} \\ 0 & (L + s_4)s\alpha_4 + HQ & 0 & -s\alpha_4 & 0 & -c\alpha_4 \\ -(L + s_4) - HQs\alpha_4 + \frac{C_3}{F_{ex}} & \frac{C_3}{F_{ey}} & -HQc\alpha_4 + \frac{C_3}{F_{ey}} & \frac{C_4}{T_{ex}} & -1 + \frac{C_4}{T_{ey}} & \frac{C_4}{T_{ez}} \\ 0 & -(L + s_4)c\alpha_4 & 0 & c\alpha_4 & 0 & -s\alpha_4 \end{bmatrix} \tag{10}$$

where the terms C_1, C_2, and C_3 are introduced to consider the weights of links, m_{HQ}, m_{QM}, m_{MM2}, and motors, m_{M4} and m_{M5}, respectively. The above-mentioned parameters can be evaluated from the Static equilibrium as

$$\begin{aligned} C_1 &= [g(m_{HQ} + m_{QM} + m_{MM2} + m_{M4} + m_{M5})]/6 \\ C_2 &= [g(m_{HQ} + m_{QM} + m_{MM2} + m_{M4} + m_{M5})]/6 \\ C_3 &= [g(-m_{M5}(0.5s_4 + L)c\alpha_4 - (0.5m_{M4}Lc\alpha_4) \\ &\quad - (m_{MM2}Lc\alpha_4))]/6 \\ C_4 &= [g(-m_{M5}(0.5s_4 + L)c\alpha_4 - (0.5m_{M4}Lc\alpha_4) \\ &\quad - (m_{MM2}Lc\alpha_4))]/6 \end{aligned} \tag{11}$$

where g is the gravity acceleration.

Because of the prismatic joint and assuming friction as negligible, the only force applied to a leg by the movable plate is that one $\mathbf{R}_k$, which is contained in the plane of the leg mechanism, as shown in Fig. 4. This is given by the components R_{ky} and R_{kz} with respect to the k-frame fixed with the linkage plane since $R_{kx} \neq 0$ will determine the sliding of the prismatic joint to a static equilibrium yet. Thus the components R_{ky} and R_{kz} will balance the force $\mathbf{F}$ and the torque $\mathbf{N}$ acting on the movable plate in agreement with the model in Fig. 4.

The reactions on each leg of the parallel manipulator, Fig. 4, can be obtained by the static equilibrium as a function of $\mathbf{F}_H = [\mathbf{F}, \mathbf{N}]$ as,[23]

$$\mathbf{F}_H = M_{FN}\mathbf{R} \tag{12}$$

where $\mathbf{R} = [R_{1x}, R_{1z}, R_{2x}, R_{2z}, R_{3x}, R_{3z}]^t$ and t is the transpose operator. The matrix M_{FN} can be written as

$$M_{FN} = \begin{bmatrix} s\delta_1 & 0 & s\delta_2 & 0 & s\delta_3 & 0 \\ c\delta_1 & 0 & c\delta_2 & 0 & c\delta_3 & 0 \\ 0 & 1 & 0 & 1 & 0 & 1 \\ 0 & r_1 s\delta_1 & 0 & r_2 s\delta_2 & 0 & r_3 s\delta_3 \\ 0 & r_1 c\delta_1 & 0 & r_2 c\delta_2 & 0 & r_3 c\delta_3 \\ r_1 & 0 & r_2 & 0 & r_3 & 0 \end{bmatrix} \tag{13}$$

in which δ_1, δ_2, δ_3 are the angles that gives the location of each leg of the parallel manipulator in the OXYZ frame; r_1, r_2 and r_3 define the application points of R_1, R_2, R_3; $s\delta_1$ is for $\sin\delta_1$, $c\delta_1$ is for $\cos\delta_1$, and so on for other angles.

The static equilibrium of a compliant CaPaMan k-leg can be expressed by referring to the equilibrium of the coupler in the form (Fig. 3)

$$[R_{ky} \quad R_{kz} \quad 0]^t = K_{Lk}[\Delta b_k \quad \Delta d_k \quad \Delta\alpha_k]^t \tag{14}$$

where the leg stiffness matrix K_{Lk} can be given by the expression of the static equilibrium of the deformed linkage

$$K_{Lk} = \begin{bmatrix} k_{bk}\, c\alpha_k & k_{dk}\, c\beta_k & -(k_{Tk}/b_k)s\alpha_k \\ k_{bk}\, s\alpha_k & k_{dk}\, s\beta_k & (k_{Tk}/b_k)c\alpha_k \\ k_{bk}\, r_{bk} & -k_{dk}\, r_{dk} & (k_{Tk}/b_k)r_{Tk} \end{bmatrix} \tag{15}$$

with

$$\begin{aligned} r_{bk} &= (c_k/2)\sin(\alpha_k + \gamma_k) + h_k \cos(\alpha_k + \gamma_k) \\ r_{dk} &= -(c_k/2)\sin(\alpha_k + \beta_k) + h_k \cos(\alpha_k + \beta_k) \\ r_{Tk} &= (c_k/2)\cos(\alpha_k - \gamma_k) + h_k \sin(\alpha_k - \gamma_k) \end{aligned} \tag{16}$$

https://doi.org/10.1017/S0263574704000323 Published online by Cambridge University Press

in which K_{bk}, K_{ck}, K_{dk}, K_{hk} are the stiffness of the links b_k, c_k, d_k, h_k, respectively, and K_{Tk} is the stiffness of the motors as shown in Fig. 4. Referring to the prototype of Fig. 1 and its scheme of Fig. 3, the stiffness parameters k_{bk} and k_{dk} can be assumed as

$$k_{bk} = k_{dk} = EA/L \tag{17}$$

where A is the cross-section area and L is the length of the link rod; E is the Young module.

The stiffness parameter k_{Tk} can be computed by using the following empirical expression for dc motors as proposed in reference [27],

$$k_{Tk} = \frac{1}{\omega_0\, \nu \tau_e} \tag{18}$$

with

$$\tau_e = \frac{L_r}{R_r}; \qquad \nu = \frac{\left(\frac{e}{\Omega} - I_0\right) K_M}{\omega_0} \tag{19}$$

where ω_0 is the no load angular velocity, R_r, L_r, e, Ω and K_M are the terminal resistance, the inductance, the voltage, the resistance and the torque constant of the dc motor, respectively.

Because of the geometry and size of CaPaMan prototype, small deformations of links can be assumed to give $\alpha_k = \beta_k$. Thus, the γ_k angle can be computed by

$$\sin\gamma_k = [(b_k + \Delta b_k)\sin\alpha_k - (d_k + \Delta d_k)\sin\beta_k]/c_k \tag{20}$$

Consequently, the coordinate variation in the leg mechanism can be computed by

$$[\Delta x_k \quad \Delta z_k \quad \Delta\gamma_k]^t = C_k[\Delta b_k \quad \Delta d_k \quad \Delta\alpha_k]^t \tag{21}$$

where

$$C_k = \begin{bmatrix} c\alpha_k - \frac{c_k - 2h_k}{2c_k} s\alpha_k & \frac{c_k - 2h_k}{2c_k} s\alpha_k & -b_k \frac{3c_k - 2h_k}{2c_k} \\ \frac{3c_k - 2h_k}{2c_k} s\alpha_k & -\frac{c_k - 2h_k}{2c_k} s\alpha_k & b_k \frac{3c_k - 2h_k}{2c_k} \\ \frac{s\alpha_k}{c_k} & -\frac{s\alpha_k}{c_k} & \frac{b_k}{c_k} \end{bmatrix} \tag{22}$$

A C_p 6×6 matrix can be defined to give the displacement variation as function of the deformation of the links in the leg mechanism in the form

$$C_p = \begin{bmatrix} C_{p1} & 0 & 0 \\ 0 & C_{p2} & 0 \\ 0 & 0 & C_{p3} \end{bmatrix} \tag{23}$$

where C_{pk} $(k = 1, 2, 3)$ is a 2×2 submatrix of C_k in Eq. (22) that has been obtained by extracting first and second rows and columns from C_k.

The overall stiffness K_p of the CaPaMan legs system can be formulated as

$$K_p = \begin{bmatrix} K_{p1} & 0 & 0 \\ 0 & K_{p2} & 0 \\ 0 & 0 & K_{p3} \end{bmatrix} \tag{24}$$

where K_{pk} $(k = 1, 2, 3)$ is a 2×2 submatrix of K_{Lk} in Eq. (15) that has been obtained by extracting first and second rows and columns from K_{Lk}.

Useful expressions have been deduced for the Direct Kinematics by using a suitable analysis procedure with a vector and matrix formulation to give[25] the coordinates of the centre point H of MP as

$$\begin{aligned} x &= \frac{y_3 - y_2}{\sqrt{3}} - \frac{r_p}{2}(1 - \sin\varphi)\cos(\psi - \theta) \\ y &= y_1 - r_p(\sin\psi\cos\theta + \cos\psi\sin\varphi\sin\theta) \\ z &= \frac{z_1 + z_2 + z_3}{3} \end{aligned} \tag{25}$$

and the orientation Euler angles of MP, Fig. 2, as

$$\begin{aligned} \psi &= \tan^{-1}\left[\sqrt{3}\frac{z_3 - z_2}{2z_1 - z_2 - z_3}\right] \\ \theta &= \sin^{-1}\left[2\frac{y_1 + y_2 + y_3}{3r_p(1 + \sin\varphi)}\right] - \psi \\ \varphi &= \cos^{-1}\left[\pm\frac{2}{3r_p}\sqrt{z_1^2 + z_2^2 + z_3^2 - z_1z_2 - z_2z_3 - z_1z_3}\right]; \\ &\qquad (z \geq z_1 \Rightarrow +;\, z < z_1 \Rightarrow -) \end{aligned} \tag{26}$$

Equations (25) and (26) have been expressed as a function of H_k coordinates y_k, z_k $(k = 1, 2, 3)$, which can be given from the input variable α_k as

$$\begin{aligned} y_k &= b_k\cos\alpha_k \\ z_k &= b_k\sin\alpha_k + h_k \end{aligned} \tag{27}$$

The components of the vector of compliant displacements $\Delta\mathbf{v} = [\Delta y_1, \Delta z_1, \Delta y_2, \Delta z_2, \Delta y_3, \Delta z_3]^t$ can be computed by using Eq. (27). In fact, they are the differences in the coordinates y_1, z_1, y_2, z_2, y_3, and z_3 before and after applying a static wrench $\mathbf{F_H}$. The vector $\Delta\mathbf{v}$ gives the compliant displacements of the movable plate, which can be described by the coordinate variation $\Delta\mathbf{X}_{CaPaMan} = [\Delta x, \Delta y, \Delta z, \Delta\varphi, \Delta\theta, \Delta\psi]^t$ by using the Direct Kinematic formulation of Eqs. (25) to (27) in the form

$$\mathbf{\Delta X}_{CaPaMan} = A_d\,\Delta\mathbf{v} \tag{28}$$

where

$$A_d = \begin{bmatrix} c_x & 0 & -\frac{1}{\sqrt{3}} & 0 & \frac{1}{\sqrt{3}} & 0 \\ 1 & 0 & c_y & 0 & 0 & 0 \\ 0 & \frac{1}{3} & 0 & \frac{1}{3} & 0 & \frac{1}{3} \\ c_\varphi & -\frac{2}{3r_p} & 0 & \frac{2}{3r_p} & 0 & \frac{2}{3r_p} \\ 0 & 0 & 0 & -\frac{\sqrt{3}}{c_\psi} & 0 & -\frac{\sqrt{3}}{c_\psi} \\ \frac{1}{c_\theta} & 0 & \frac{1}{c_\theta} & \frac{\sqrt{3}}{c_\psi} & \frac{1}{c_\theta} & -\frac{\sqrt{3}}{c_\psi} \end{bmatrix} \tag{29}$$

in which coefficients c_x, c_y, c_z, c_φ, c_ψ and c_θ can be evaluated by considering the expressions (25) and (26), of direct

https://doi.org/10.1017/S0263574704000323 Published online by Cambridge University Press

Table I. Design parameters of CaHyMan.

$a_k = c_k$ (mm)	$b_k = d_k$ (mm)	h_k (mm)	s_{kmax} (mm)	α_{min} (deg)	α_{max} (deg)
200	80	96	109.5	45	135
HQ (mm)	L (mm)	s_{4min} (mm)	s_{4max} (mm)	α_{4min} (deg)	α_{4max} (deg)
30	100	0	50	30	90

kinematics for computing the variations to give

$$\begin{aligned} c_x &= -(r_p/2\Delta y_1)(1-\sin\Delta\varphi)\cos(\Delta\psi-\Delta\theta) \\ c_y &= -(r_p/\Delta y_2)(\sin\Delta\varphi\cos\Delta\varphi+\cos\Delta\psi\sin\Delta\varphi\sin\Delta\theta \\ c_\varphi &= 1/\Delta y_1 \\ c_\psi &= 2\Delta z_1-\Delta z_2-\Delta z_3 \\ c_\theta &= (3r_p/2)(1+\sin\Delta\varphi) \end{aligned} \tag{30}$$

The computation of A_d needs the values of the compliant angular displacements $\Delta\varphi$, $\Delta\theta$ and $\Delta\psi$ in the coefficients of Eqs. (30). A first approach for solving this non-linearity can be outlined as a trial-and-error procedure by using Eq. (28) to verify iteratively the values of displacements $\Delta\varphi$, $\Delta\theta$ and $\Delta\psi$, that are given from the coefficients of Eqs. (30).

Alternatively, A_d can be computed by using a linearized expression

$$\Delta X_{CaPaMan} = [A'_d]\Delta v + \|\Delta v\|\varepsilon \tag{31}$$

where $[A'_d]$ is the matrix of the partial derivatives of $[A_d]$ with respect to $\Delta\mathbf{v}$ components; $\|\Delta\mathbf{v}\|$ is the norm of $\Delta\mathbf{v}$ and ε is the error depending on the size of $\Delta\mathbf{v}$.[28]

Thus, the stiffness matrix $K_{CaPaMan}$ of the parallel chain can be expressed as

$$K_{PAR} = M_{FN}\, K_P\, C_P^{-1}\, A_d'^{-1} \tag{32}$$

Therefore, the stiffness matrix K_{PAR} of Eq. (3) can be computed straightforward by using Eqs. (10) to (32).

5. A NUMERICAL EVALUATION OF STIFFNESS

The built prototype of CaHyMan in Fig. 1 has been analyzed and it can be modeled by using the stiffness parameters $K_{bk} = K_{dk} = 2.625 \times 10^6$ N/m, $K_{Tk} = 4.672 \times 10^3$ Nm/rad, $K_4 = 2.625 \times 10^6$ N/m, $K_s = 0.697$ N/m, $K_{T1} = 0.876 \times 10^3$ Nm/rad, that have been computed by using literature data for components, as in reference [27]. By using these stiffness parameters and the proposed formulation of Eqs. (1) to (32), the stiffness matrix of CaHyMan can be numerically computed with no great computational effort (Table I).

The numerically computed stiffness matrix of CaHyMan can be useful to analyze the stiffness behavior of CaHyMan. But it is necessary to define how to compare different stiffness matrices. A suitable comparison could be obtained by using the determinant, trace, or eigenvalues of the stiffness matrices.

The determinant of a stiffness matrix K can be computed as

$$\det K = (-1)^6 + S_1(-1)^5 + S_2(-1)^4 + S_3(-1)^3 + S_4(-1)^2 + S_5(-1) + S_6 \tag{33}$$

where S_i (with $i = 1, 2, \ldots, 6$) is the sum of the principal minors of order i of the matrix K, as given in matrix algebra.[28]

The trace is the sum of the diagonal elements K_{ii} (with $i = 1, 2, \ldots, 6$) of a matrix and it can be computed as,[28]

$$\mathrm{tr}\, K = k_{11} + k_{22} + k_{33} + k_{44} + k_{55} + k_{66} \tag{34}$$

The trace can be seen as the sum of the components of compliance displacements along the principal directions. In fact, if $\mathbf{F_M} = [1, 0, 0, 0, 0, 0]^t$, k_{11} will be equal to the component of compliance displacement along the X-axis. Similarly, one can write k_{22}, k_{33}, k_{44}, k_{55}, k_{66} as the other components of compliance displacement along the base frame axes. Nevertheless, it is worthy nothing that k_{11}, k_{22}, k_{33} and k_{44}, k_{55}, k_{66} do not have the same dimensions and thus the sum has not a full physical interpretation.

The eigenvalues of K can be computed as the roots of the characteristic polynomial that can be written as

$$(-\lambda)^6 + S_1(-\lambda)^5 + S_2(-\lambda)^4 + S_3(-\lambda)^3 + S_4(-\lambda)^2 + S_5(-\lambda) + S_6 = 0 \tag{35}$$

where S_i (with $i = 1, 2, \ldots, 6$) is the sum of the principal minors of order i of the matrix K.

The eigenvalues can be used to make considerations on the stability conditions as proposed in reference [29]. But they cannot describe physically the stiffness behavior of the CaHyMan in a straightforward way. Moreover, they cannot be directly compared if they have not the same eigenvectors.

Therefore, the stiffness behavior of CaHyMan can be conveniently analyzed only by using the determinant of $K_{CaHyMan}$, as proposed in reference [23]. In fact, the compliance displacement of CaHyMan can be computed as

$$\Delta X_{CaHyMan} = K_{CaHyMan}^{-1}\, F_M \tag{36}$$

and each term k_{ij}^{-1} of the inverse matrix of $K_{CaHyMan}$ can be computed as

$$k_{ij}^{-1} = \frac{(K_{CaHyMan})_{ji}}{\det K_{CaHyMan}} \tag{37}$$

where $(K_{CaHyMan})_{ji}$ is the algebraic complement of the element k_{ij} of the matrix $K_{CaHyMan}$ with $i, j = 1, 2, \ldots, 6$. Thus, if the determinant $\det K_{CaHyMan}$ is zero, the Eq. (35) gives singular values and Eq. (32) cannot be computed. Therefore, the determinant of $K_{CaHyMan}$ can be used as a performance index to investigate synthetically the effect of the design parameters on the stiffness behavior of CaHyMan, since it is easy computable and particularly significant for determining stiffness singularity properties.

By using the proposed formulation the compliant displacement of CaHyMan, which is due to the external

https://doi.org/10.1017/S0263574704000323 Published online by Cambridge University Press

Table II. Compliant displacements of CaHyMan when $\alpha_1 = \alpha_2 = \alpha_3 = \alpha_4 = 90$ deg. and $s_4 = 50$ mm.

$\Delta \mathbf{X}_{\text{CaHyMan}}$	$\mathbf{Fe} = (1.0; 1.0; 1.0)^t$ $\mathbf{Ne} = (0.0; 0.0; 0.0)^t$ [N; Nm]	$\mathbf{Fe} = (0.0; 0.0; 0.0)^t$ $\mathbf{Ne} = (1.0; 1.0; 1.0)^t$ [N; Nm]	$\mathbf{Fe} = (1.0; 1.0; 1.0)^t$ $\mathbf{Ne} = (1.0; 1.0; 1.0)^t$ [N; Nm]
Δx [mm]	0.10	−0.50	−0.50
Δy [mm]	0.01	0.01	0.01
Δz [mm]	0.37	−3.07	−2.70
$\Delta \varphi$ [deg]	−0.92	−0.85	−0.74
$\Delta \psi$ [deg]	0.84	1.52	1.33
$\Delta \theta$ [deg]	−0.57	0.99	0.66

force $\mathbf{F_e}$ and torque $\mathbf{N_e}$, can be numerically computed through Eqs. (2) to (32). Tables II, III and IV show the computed values of the components the compliant displacement of CaHyMan when $\alpha_1 = \alpha_2 = \alpha_3 = \alpha_4 = 90$ deg. and $s_4 = 50$ mm, when $\alpha_1 = \alpha_2 = \alpha_3 = \alpha_4 = 30$ deg. and $s_4 = 0$ mm, when $\alpha_1 = 45$ deg., $\alpha_2 = 60$ deg., $\alpha_3 = 75$ deg., $\alpha_4 = 45$ deg. and $s_4 = 0$ mm, respectively. Tables II, III and IV give the maximum compliance displacement of CaHyMan in the analyzed configurations and under different external loads, and it has been computed as few millimeters and few degrees.

The components of the compliant displacement have been also computed as a function of the external force $\mathbf{F_e}$ and torque $\mathbf{N_e}$, and the results are reported in Figs. 5 and 6, respectively. In particular, Fig. 5 gives the compliant displacements of CaHyMan as a function of $F_{ex} = F_{ey} = F_{ez}$ when $N_{ex} = N_{ey} = N_{ez} = 0$ when the manipulator is in a configuration in which $\alpha_1 = \alpha_2 = \alpha_3 = \alpha_4 = 60$ deg. and $s_4 = 50$ mm. Figures 5(a), (b) and (c) give the linear compliant displacements along the X, Y and Z axes versus the external force $\mathbf{F_e}$, respectively. It is worthy to note that in these plots the modules of the compliant displacements are linear functions of $\mathbf{F_e}$. Figure 5(d), (e) and (f) give the angular compliant displacements in term of the φ, ψ, and θ angles as non linear functions of the external force $\mathbf{F_e}$, respectively.

Similarly, Fig. 6 gives the compliant displacements of CaHyMan as a function of $N_{ex} = N_{ey} = N_{ez}$ when $F_{ex} = F_{ey} = F_{ez} = 0$ when the manipulator is in a configuration in which $\alpha_1 = \alpha_2 = \alpha_3 = \alpha_4 = 60$ deg. and $s_4 = 50$ mm. Also in this case the modules of linear compliant displacements along the X, Y and Z axes are linear functions of $\mathbf{N_e}$, as shown in Fig. 6(a), (b) and (c), respectively, and the angular compliant displacements in term of the φ, ψ, and θ angles are non linear functions of the external force $\mathbf{N_e}$, as shown in Fig. 6(d), (e) and (f), respectively. It is worthy to note that there are compliant displacements also when $F_{ex} = F_{ey} = F_{ez} = 0$ and $N_{ex} = N_{ey} = N_{ez} = 0$, as shown in Figs. 5a), d), e), f), and in Figs. 6d), e), f) since in a general configuration of the manipulator the weight of the links exerts an action as an external force.

Table III. Compliant displacements of CaHyMan when $\alpha_1 = \alpha_2 = \alpha_3 = \alpha_4 = 30$ deg. and $s_4 = 0$ mm.

$\Delta \mathbf{X}_{\text{CaHyMan}}$	$\mathbf{Fe} = (1.0; 1.0; 1.0)^t$ $\mathbf{Ne} = (0.0; 0.0; 0.0)^t$ [N; Nm]	$\mathbf{Fe} = (0.0; 0.0; 0.0)^t$ $\mathbf{Ne} = (1.0; 1.0; 1.0)^t$ [N; Nm]	$\mathbf{Fe} = (1.0; 1.0; 1.0)^t$ $\mathbf{Ne} = (1.0; 1.0; 1.0)^t$ [N; Nm]
Δx [mm]	−0.50	7.60	7.10
Δy [mm]	−0.40	6.30	5.90
Δz [mm]	−0.40	5.70	5.30
$\Delta \varphi$ [deg]	−1.01	3.04	2.87
$\Delta \psi$ [deg]	0.97	−2.49	−2.35
$\Delta \theta$ [deg]	−0.08	0.21	0.65

Table IV. Compliant displacements of CaHyMan when $\alpha_1 = 45$ deg., $\alpha_2 = 60$ deg., $\alpha_3 = 75$ deg., $\alpha_4 = 45$ deg. and $s_4 = 0$ mm.

$\Delta \mathbf{X}_{\text{CaHyMan}}$	$\mathbf{Fe} = (1.0; 1.0; 1.0)^t$ $\mathbf{Ne} = (0.0; 0.0; 0.0)^t$ [N; Nm]	$\mathbf{Fe} = (0.0; 0.0; 0.0)^t$ $\mathbf{Ne} = (1.0; 1.0; 1.0)^t$ [N; Nm]	$\mathbf{Fe} = (1.0; 1.0; 1.0)^t$ $\mathbf{Ne} = (1.0; 1.0; 1.0)^t$ [N; Nm]
Δx [mm]	0.01	−0.30	−0.20
Δy [mm]	0.01	−0.10	−0.10
Δz [mm]	0.01	−0.20	−0.20
$\Delta \varphi$ [deg]	−0.79	0.22	0.34
$\Delta \psi$ [deg]	0.78	−0.21	−0.33
$\Delta \theta$ [deg]	9.34	0.43	−2.54

https://doi.org/10.1017/S0263574704000323 Published online by Cambridge University Press

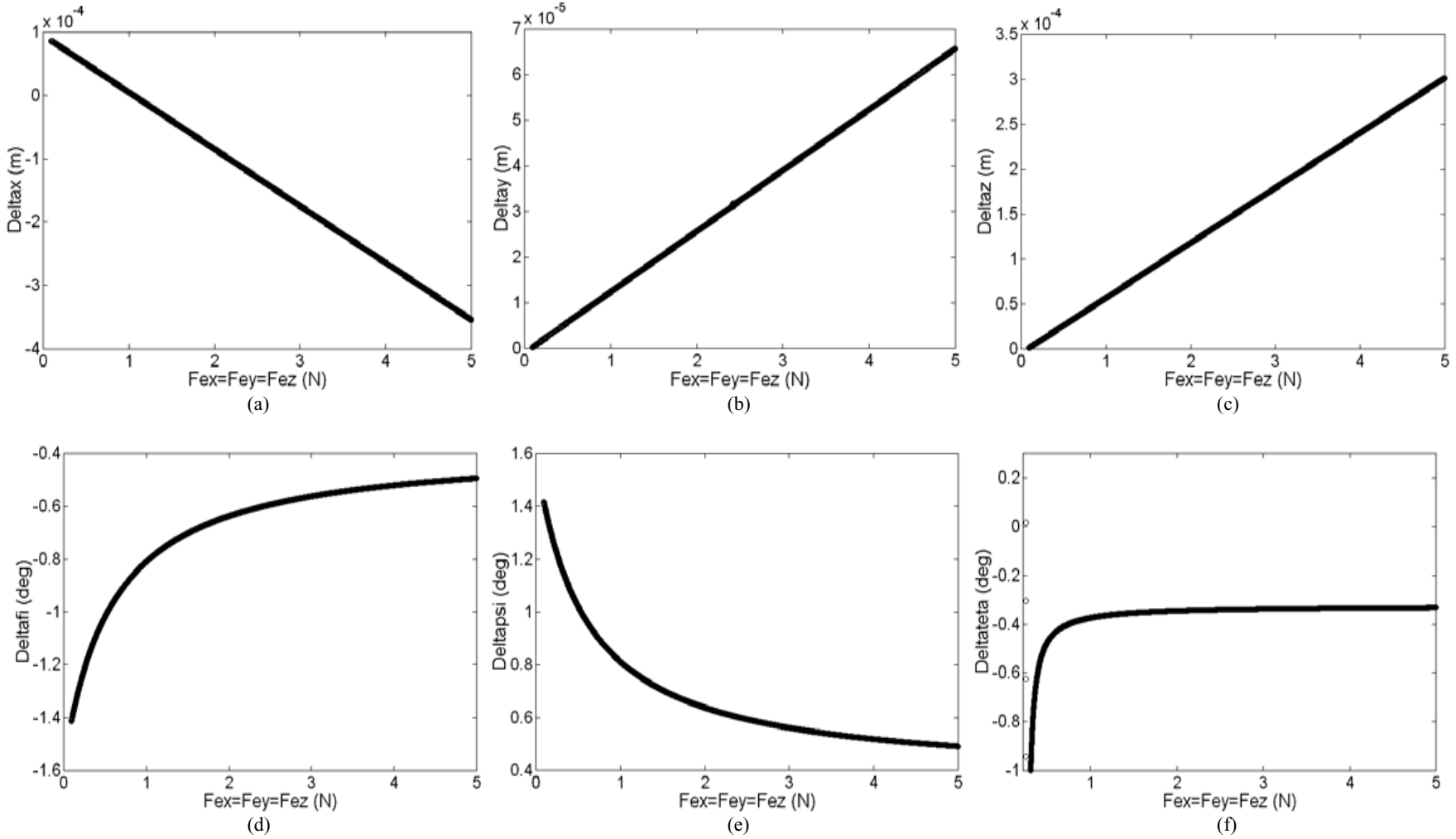

Fig. 5. Compliant displacements of CaHyMan as a function of $F_{ex} = F_{ey} = F_{ez}$ when $N_{ex} = N_{ey} = N_{ez} = 0$ for $\alpha_1 = \alpha_2 = \alpha_3 = \alpha_4 = 60$ deg. and $s_4 = 50$ mm: (a) Δx; (b) Δy; (c) Δz; (d) $\Delta\varphi$; (e) $\Delta\psi$; (f) $\Delta\theta$.

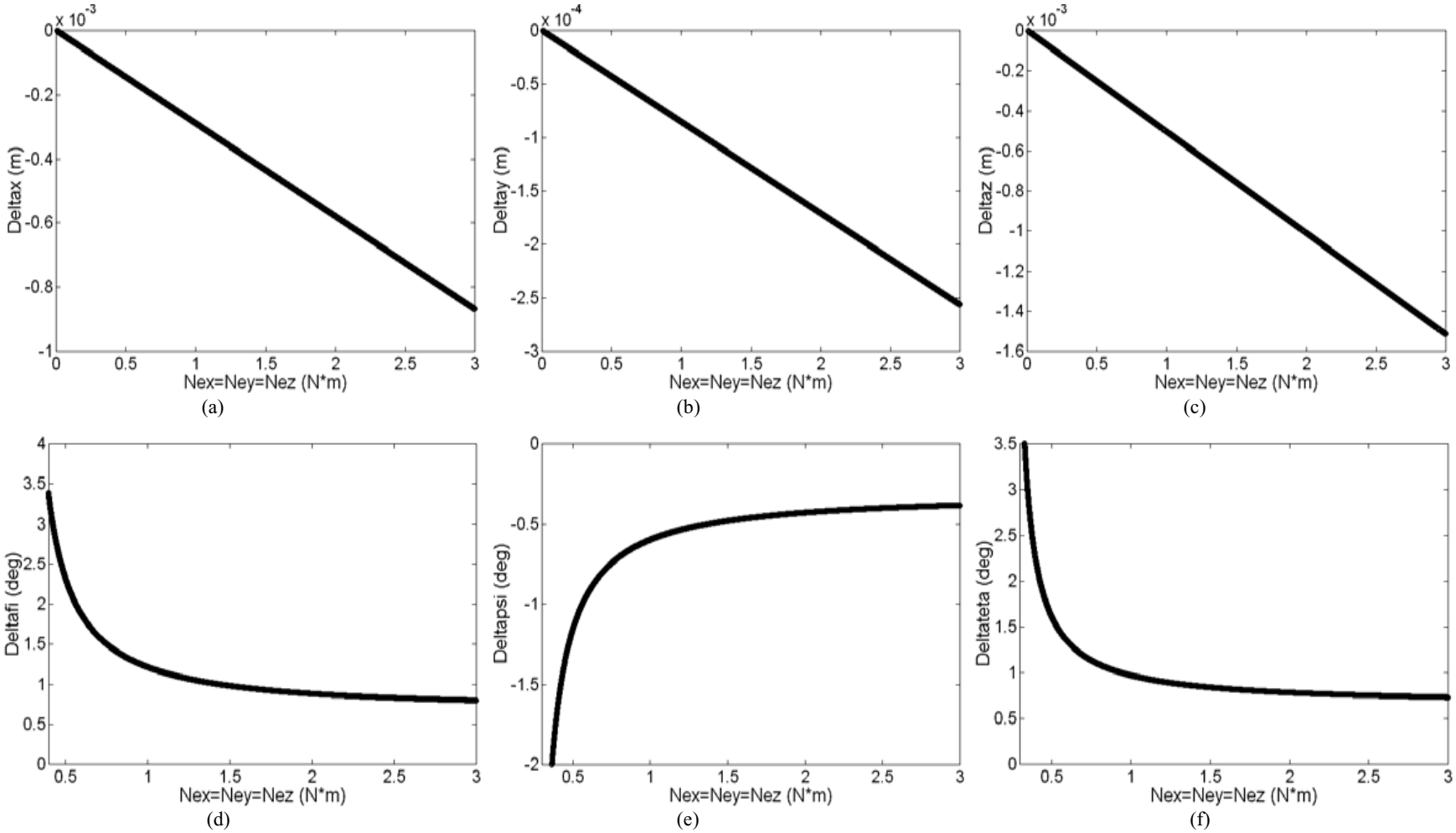

Fig. 6. Compliant displacements of CaHyMan as a function of $N_{ex} = N_{ey} = N_{ez}$ when $F_{ex} = F_{ey} = F_{ez} = 0$ for $\alpha_1 = \alpha_2 = \alpha_3 = \alpha_4 = 60$ deg. and $s_4 = 50$ mm: (a) Δx; (b) Δy; (c) Δz; (d) $\Delta\varphi$; (e) $\Delta\psi$; (f) $\Delta\theta$.

6. CONCLUSION

The main contribution of this paper consists in presenting the basic mechanical stiffness characteristics of a 5 d.o.f. parallel-serial manipulator, named CaHyMan (Cassino Hybrid Manipulator), and in proposing a formulation with closed-form expressions, due to the triangular assembly of the three legs and specific geometry of leg mechanisms with parallelogram linkages in its chain. The proposed analysis is specific for the CaHyMan architecture, but the approach and procedure can be adopted by general features for stiffness analysis of hybrid manipulators with serial and parallel architectures.

The stiffness behavior of the manipulator CaHyMan has been investigated by using proper schemes in order to obtain a closed-form formulation. By using the proposed formulation the stiffness matrix and compliant displacement of CaHyMan have been numerically computed for several configurations of the manipulator. The satisfactory results confirm that CaHyMan is able to operate with high performance in static or quasi-static operations.

At the Laboratory of Robotics and Mechatronics in Cassino, Italy, experimental tests are undergoing with the built prototype for practical validation and further investigation of characteristics and feasible applications by using the results of herein proposed numerical characterization.

References

1. Staubli robot division webpage, http://www.staubli.com/web/robot/division.nsf, (2003).
2. Fanuc Robotica homepage http://www.fanucrobotics.com, (2003).
3. Toshiba Machine Co. homepage, http://www.toshiba-machine.com, (2003).
4. ABB homepage, http://www.abb.com, (2003).
5. J.-P. Merlet, *Les Robots Paralleles* (Hermes, Paris, 1997).
6. O. Khatib, B. Roth and K. J. Waldron, "The Design of a High-Performance Force-Controlled Manipulator," *8th World Congress on the Theory of Machines and Mechanisms*, Prague (1991), **Vol. 2**, pp. 475–478.
7. B. O. Choi, M. K. Lee and K. W. Park, "Kinematic and Dynamic Models of Hybrid Robot Manipulator for Propeller Grinding," *Journal of Robotic Systems* **16**, No. 3, 137–150 (1999).
8. H. K. Tonchoff, G. Gunther and H. Grendel, "Vergleichende Betrachtung paralleler und hybrider Strukturen," *Proceedings of Conference on New Machine Concepts for Handling and Manufacturing Devices on the Basis of Parallel Structures* VDI N. 1427, Braunschweig (1998) pp. 249–270.
9. H. H. Cheng, "Real-Time Manipulation of a Hybrid Serial-and-Parallel-Driven Redundant Industrial Manipulator," *ASME Journal of Dynamic Systems, Measurement, and Control* **116**, 687–701 (1994).
10. M. Shahinpoor, "Kinematics of a Parallel-Serial (Hybrid) Manipulator," *Journal of Robotic Systems* **9**, No. 1, 17–36 (1992).
11. L. Romdhane, "Design and Analysis of a Hybrid Serial-Parallel Manipulator," *Mechanism and Machine Theory* **34**, 1037–1055 (1999).
12. W. K. Kim, S. Tosunoglu and B. J. Yi, "Geometric/Kinematic Characteristics of 6 Degree-of-Freedom Hybrid Mechanisms with Forward Closed-Form Position Solutions," *World Automation Congress ISORA'98*, Albuquerque (1998) paper n.ISORA-070.
13. K. Nazarczuk, K. Mianowski, A. Oledzki and C. Rzymkowski, "Experimental Investigation of the Robot's Arm with Serial-Parallel Structure," *Proceedings of 9th World Congress on the Theory of Machines and Mechanisms*, Milan (1995) pp. 2112–2116.
14. M. Z. Huang and S-H. Ling, "Kinematics of a Class of Hybrid Robotic Mechanisms with Parallel and Series Module," *IEEE International Conference on Robotics and Automation ICRA'94*, San Diego (1994) pp. 2180–2185.
15. K. E. Zanganeh and J. Angeles, "Displacement Analysis of a Six-Degree-of-Freedom Hybrid Hand Controller," *IEEE International Conference on Robotics and Automation ICRA'96*, Minneapolis (1996) pp. 1281–1286.
16. S. L. Wang, "On Force and Motion Control of Serial-Parallel Robots," *Proceedings of ASME Design Engineering Technical Conferences and Computers in Engineering Conference*, Irvine (1996) pp. 1–7.
17. J. Duffy, *Statics and Kinematics with Applications to Robotics* (Cambridge University Press, Cambridge, 1996) pp. 153–169.
18. C. M. Gosselin and D. Zhang, "Stiffness Analysis of Parallel Mechanisms Using a Lumped Model," *Int. J. Robotics and Automation* **17**, No. 1, 17–27 (2002).
19. L. W. Tsai, *Robot Analysis: The Mechanics of Serial and Parallel Manipulators* (John Wiley & Sons, New York, 1999) pp. 260–297.
20. T. Pigoski, M. Griffis and J. Duffy, "Stiffness Mappings Employing Different Frames of Reference". *Mechanism and Machine Theory* **33**, No. 6, 825–838 (1998).
21. W. K. Yoon, T. Suehiro, Y. Tsumaki and M. Uchiyama, "A Method for Analyzing Parallel Mechanism Stiffness Including Elastic Deformations in the Structure," *Proceedings of the IEEE/RSJ International Conference on Intelligent Robots and Systems IROS'02*, Lausanne (2002) pp.2875–2880.
22. M. Ceccarelli and G. Carbone, "A Stiffness Analysis for CaPaMan (Cassino Parallel Manipulator)," *Mechanism and Machine Theory* **37**, No. 5, 427–439 (2002).
23. M. Ceccarelli, G. Carbone and M. Teolis, "A Numerical Evaluation of the Stiffness of CaHyMan (Cassino Hybrid Manipulator)," *Proceedings of 2nd Workshop on Computational Kinematics CK 2001*, Seoul (2001) pp. 145–154; *Electronic Journal of Computational Kinematics EJCK*, http://www-sop.inria.fr/coprin/EJCK/EJCK.html, **1**, No. 1, Paper No. 14 (2002).
24. G. Carbone, "Stiffness Evaluation of Multibody Robotic Systems," *PhD Dissertation* (University of Cassino, Cassino, Italy, 2003).
25. M. Ceccarelli, "A New 3 dof Spatial Parallel Mechanism," *Mechanism and Machine Theory* **32**, No. 8, 895–902 (1997).
26. M. Ceccarelli and G. Figliolini, "Mechanical Characteristics of CaPaMan (Cassino Parallel Manipulator)," *Proceedings of 3rd Asian Conference on Robotics and its Applications*, Tokyo (1997) pp. 301–308.
27. E. I. Rivin, *Stiffness and Damping in Mechanical Design* (Marcel Dekker Inc., New York, 1999).
28. F. R. Gantmacher, *The Theory of Matrices*. Chelsea Publishing Company, New York, (1989) **vol. 1**.
29. M. Svinin, S. Hosoe and M. Uchiyama, "On the Stability and Stabilizability of Elastically Suspended Rigid Bodies," *Proceedings of 2nd Workshop on Computational Kinematics CK 2001* Seoul (2001) pp. 155–166.

https://doi.org/10.1017/S0263574704000323 Published online by Cambridge University Press